Taylor & Francis
Taylor & Francis Group

Hydrological Sciences Journal

ISSN: 0262-6667 (Print) 2150-3435 (Online) Journal homepage: http://www.tandfonline.com/loi/thsj20

Climate change impacts on streamflow and sediment yield in the North of Iran

Mahmood Azari, Hamid Reza Moradi, Bahram Saghafian & Monireh Faramarzi

HYDROLOGICAL SCIENCES JOURNAL – JOURNAL DES SCIENCES HYDROLOGIQUES, 2016
VOL. 61, NO. 1, 123–133
http://dx.doi.org/10.1080/02626667.2014.967695

Climate change impacts on streamflow and sediment yield in the North of Iran

Mahmood Azari[a], Hamid Reza Moradi[a], Bahram Saghafian[b] and Monireh Faramarzi[c,d]

[a]Department of Watershed Management Engineering, College of Natural Resources, Tarbiat Modares University (TMU), Noor, Mazandaran Province, Iran; [b]Department of Technical and Engineering, Science and Research Branch, Islamic Azad University, Tehran, Iran; [c]Department of Natural Resources, Isfahan University of Technology, Isfahan, Iran; [d]University of Alberta Water Initiative, University of Alberta, Edmonton, Alberta, T6G 2E9, Canada

ABSTRACT

Climate change will accelerate the hydrological cycle, altering rainfall, and the magnitude and timing of runoff. The purpose of this paper is to assess the impacts of climate change on streamflow and sediment yield from the Gorganroud river basin in the North of Iran. To study the effects of climatic variations, the SWAT model was implemented to simulate the hydrological regime and the SUFI-2 algorithm was used for parameter optimization. The climate change scenarios were constructed using the outcomes of three general circulation models for three emission scenarios. The study results for 2040–2069 showed an increase in annual streamflow of 5.8%, 2.8% and 9.5% and an increase in sediment yield of 47.7%, 44.5% and 35.9% for the A1F1, A2 and B1 emission scenarios, respectively. This implies that the impact of climate change on sediment yield is greater than on streamflow. Monthly variations show that the increase in discharge and sediment yield is more pronounced in wet seasons and the decrease is more pronounced in summer (July–September). The results highlighted the strong impact of climate change and reflected the importance of incorporating such analysis into adaptive management.

ARTICLE HISTORY
Received 7 January 2014
Accepted 12 September 2014

EDITOR
Z.W. Kundzewicz

ASSOCIATE EDITOR
Not assigned

KEYWORDS
Climate change; hydrological impacts assessment; SWAT; streamflow; sediment yield; iran

Introduction

The consensus of atmospheric scientists is that the Earth is warming and as global temperatures increase the hydrological cycle is becoming more vigorous. The Intergovernmental Panel on Climate Change (IPCC) has reported with virtual certainty (probability N99%) that both land and sea surface temperatures have increased by 0.4–0.7°C since the late 19th century (Nearing *et al.* 2005). According to the Fourth Assessment Report (AR4) of the IPCC, global mean surface temperature, precipitation and extreme events such as heavy precipitation and droughts have changed significantly, and the changes are very likely to continue (IPCC 2007). The rise in Earth near-surface air temperature and changes in precipitation patterns are prominent features of climate change; these two factors impact almost all other hydrological processes. All atmospheric ocean general circulation models (AOGCMs) predict a rise in Earth surface temperature and rainfall intensity and amount due to increases in greenhouse gas (GHG) concentration over the coming century (Kaini *et al.* 2010).

A warmer climate will accelerate the hydrological cycle, altering rainfall and the magnitude and timing of runoff. Changes in climate are also expected to have noticeable effects on the soil since rainfall and runoff are the factors controlling soil erosion and sediment transport within landscapes. The changes in flow characteristics resulting from climate change depend on individual catchment characteristics. In particular, basin geology and elevation are first-order controls on the timing and magnitude of basin runoff to climate change (Hamlet and Lettenmaier 2007). Reliable predictions of the quantity and rate of runoff, and sediment transport are needed to help decision makers in developing watershed management plans for better soil and water conservation measures.

Many recent studies have focused on the potential effects of climate change on water quality and quantity. Muttiah and Wurbs (2002) used SWAT to simulate the impacts of climate change for the San Jacinto River basin in Texas. They reported that the climate change scenarios resulted in a higher mean stream discharge which might induce greater flooding, but the frequency of the normal and low stream discharges decreased. Gosain *et al.* (2006) simulated the impacts of a 2041–2060 climate change scenario on stream discharges from 12 major river basins in India. Stream

CONTACT: Hamid Reza Moradi hrmoradi1340@yahoo.com

discharge was found to generally decrease, and the severity of both floods and droughts increased in response to the climate change projection. To predict streamflow in the upper Mississippi River basin, Jha *et al.* (2006) used various global climate models. Study results showed a wide range of changes, from a 6% decrease to a 51% increase depending primarily on precipitation patterns. Abbaspour *et al.* (2009) used this calibrated hydrological model to study the impact of future climate on water availability in Iran. Future climate scenarios for periods of 2010–2040 and 2070–2100 were generated from the Canadian Global Coupled Model (CGCM 3.1) for scenarios A1B, B1, and A2. Analysis of daily rainfall intensities indicated more frequent and larger-intensity floods in the wet regions and more prolonged droughts in the dry regions. Chang and Jung (2010) estimated potential changes in annual and seasonal trends of high flow and low flow and associated uncertainty in the 218 sub-basins of the Willamette River basin of Oregon. The seasonal variability of runoff is projected to increase consistently with increases in winter flow and decreases in summer flow. Zarghami *et al.* (2011) used the LARS-WG and general circulation models (GCMs) outputs to predict climate change in the East Azerbaijan Province in Iran. The research outcomes showed dramatic reductions in flows.

Various studies have been performed to determine the effects of climate change on soil erosion and sediment yield. The influence of climate change on suspended sediment transport in Danish rivers was studied by Thodsen *et al.* (2008) using the HIRHAM regional climate model. Results incorporating projected changes in land use/land cover for the period 2071–2100 showed an increase in suspended sediment transport in the winter months as a result of the increase in river discharge, and decreases during summer and early autumn months. Phan *et al.* (2011) used the SWAT model to simulate the impacts of climate change on stream discharge and sediment yield from the Song Cau watershed in Vietnam. The results showed that the highest changes in stream discharge (up to 11.4%) and sediment load (up to 15.3%) can be expected in wet seasons in the 2050s according to the high-emission scenario (A2), while for the low-emission scenario the corresponding changes are 8.8% and 12.6%. Li *et al.* (2011) using SWAT model simulations in the lower Pearl River basin, South China, concluded that a 3°C increase in average annual air temperature would increase the sediment load by about 13%. Mukundan *et al.* (2013) used the SWAT-water balance (SWAT-WB) model and nine GCMs to simulate potential climate change impacts on soil erosion and suspended sediment yield in the Cannonsville watershed, in New York City. Analysis of seasonal changes showed that future climate-related changes in soil erosion and sediment yield were more significant in the winter due to a shift in the timing of snowmelt and also due to a decrease in the proportion of precipitation received as snow. Although an increase in future summer precipitation was predicted, soil erosion and sediment yield appeared to decrease owing to an increase in soil moisture deficit and a decrease in water yield due to increased evapotranspiration. Shrestha *et al.* (2013) evaluated the impact of climate change on sediment yield in the Nam Ou basin located in northern Laos using future climate data from four GCMs and SWAT. Study results showed that the changes in annual stream discharges are likely to range from a 17% decrease to a 66% increase in the future, which will lead to predicted changes in annual sediment yield ranging from a 27% decrease to about a 160% increase.

The above studies indicate that watershed processes are very sensitive to changes in precipitation and temperature, and the intensity and characteristics of the impact can vary significantly from region to region. Considering all regions of the world are expected to experience a net negative impact due to climate change, quantifying hydrological impacts will be valuable in understanding and predicting sediment yield and discharge processes. Understanding the potential future changes in sediment load also should be seen as an important requirement for sound river basin management. Therefore, in this study we aimed to evaluate the potential impacts of climate change on streamflow and sediment yield in the Gorganroud River basin in northern Iran. For this the SWAT model and climate change projection from three GCMs (CGCM2, CSIRO2 and HadCM3) for the time period 2040–2069 under the A1F1, A2 and B1 GHG emissions scenarios were used. The wide range of SWAT applications demonstrates that the model is a flexible and robust tool that can be used to simulate a variety of watershed problems. Hence, SWAT was selected for this study because of its ability to simulate regional water flow at a watershed scale and to provide effective results. This paper contributes to the scientific understanding of changing sediment yield and streamflow and offers baseline information for adaptive soil and water resource management in a changing climate.

Material and methods

Study area

The 7 138 km^2 Gorganroud River basin is located in the North of Iran, between 36° 43′–37° 49′ N and 54° 42′–56° 28′ E (Fig. 1). The watershed has a general slope to the north west. Agriculture, range lands and forests dominate the land use. The elevation ranges from 10 m at the outlet to 2898 m at the top of the highlands in the south west of the watershed. Using De Martonne's aridity index, which is the ratio between the mean annual values of precipitation (P) and temperature (T) plus 10°C (De Martonne 1926), the climate in the Gorganroud is semi-arid in the eastern and wet in the western parts. The annual rainfall varies from 231 mm to 848 mm. The minimum and maximum temperatures in the basin are 11°C and 18.1°C, respectively. Annual streamflow in the Gorganroud station located at the outlet is 14.3 m^3/s, varying from 3.2 m^3/s in March to 41.8 m^3/s in September. The watershed geology in the mountain area generally consists of Jurassic limestone, schist and loess deposits. The western part of the watershed is underlain by the Quaternary deposits in the lower reaches of the main river. Soil erosion and high sediment yields, floods and debris flow are serious problems in the Gourganroud river basin. High rainfall events where soils are sensitive to erosion combined with intensive land use change (from range lands and forest to dry lands) have caused more runoff and subsequently high soil losses and sediment yield in the watershed (LarConsultingEngineering 2007).

The SWAT model

The SWAT is a physical-process-based model which simulates continuous-time landscape processes at a catchment scale (Arnold *et al.* 1998). In SWAT, each watershed is divided into hydrological response units (HRUs) based on soil type, land use and slope classes which allows a high level of spatial detail simulation. The major model components include hydrology, weather, soil erosion, nutrients, soil temperature, crop growth, pesticides, agricultural management and stream routing. The model predicts the hydrology at each HRU using a water balance equation, which includes daily precipitation, runoff, evapotranspiration, percolation and return flow components. The surface runoff is estimated in the model using two options: (a) the Natural Resources Conservation Service Curve Number (CN) method, and (b) the Green and Ampt method. The percolation through each soil layer is predicted using storage routing techniques combined with a crack-flow model. The evapotranspiration is estimated in SWAT using three approaches: (i) Priestley-Taylor, (ii) Penman-Monteith and (iii) Hargreaves. The flow routing in the river channels is computed using the variable storage coefficient method, or the Muskingum method (Arnold *et al.* 1998). The SWAT model simulates soil erosion and sediment export from hillslopes as well as in-stream channel processes. Erosion caused by rainfall and runoff is calculated with the modified universal soil loss equation (MUSLE) (for more details see Neitsch *et al.* 2005).

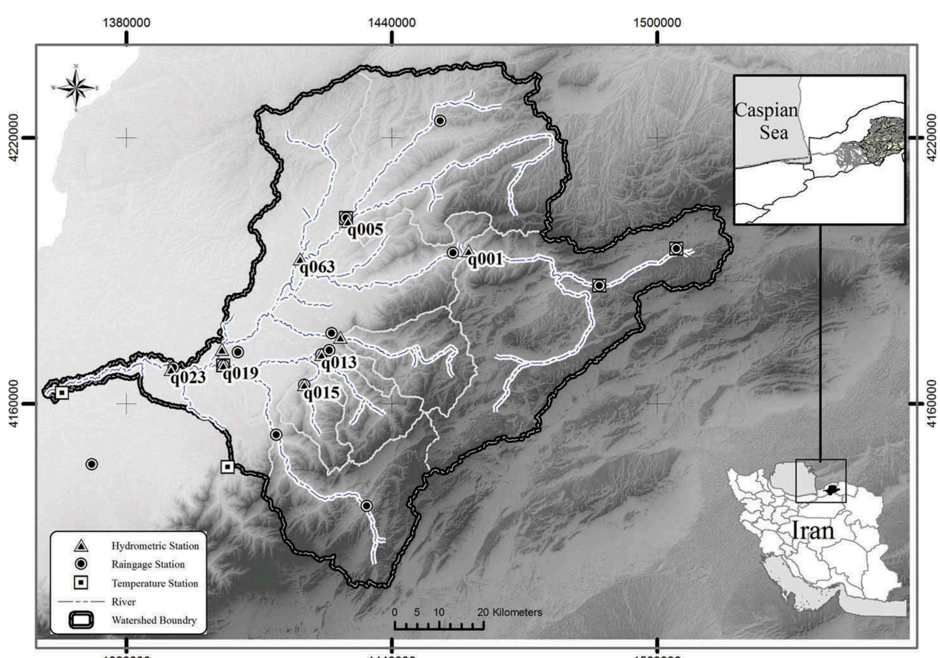

Figure 1. Location of the Gorganroud watershed in Iran.

Input data and model set-up

Hydro-climatological and topographical data were obtained from various sources for calibration and validation of the hydrological model. The land-use map extracted from Landsat thematic mapper (TM) satellite imagery with a resolution of 30 m was further interpreted based on field investigation. The map represents seven different land-use classes. The soil map was obtained from the Iranian Ministry of Agriculture. It has a spatial resolution of 1:250 000 and includes a set of physical and chemical soil properties for different layers of the soil. The watershed area of the Gorganroud was delineated and discretized into subbasins using a 90-m digital elevation model (http://srtm.csi.cgiar.org). Daily observed climate data including daily precipitation and temperature were obtained for 15 stations from the Iranian Meteorological Organization and the WRMO of Iran. River daily discharge data required for calibration/validation were obtained from the WRMO of Iran. The monthly discharge data from eight hydrometric stations and the monthly sediment loads predicted by a rating curve as a function of mean daily streamflow for 23 years were used for model calibration and validation. Using the above data a threshold value of 5000 ha was selected to delineate the watershed area. Five slope classes including 0–5, 5–12, 12–30 and 30–60 were used in the HRU definition. With these specifications a total of 79 subbasins and 554 HRUs were delineated in the study area.

Calibration and sensitivity analysis

Uncertainty and sensitivity analysis were performed using the Sequential Uncertainty Fitting Program (SUFI-2) in the SWAT-CUP package (Abbaspour 2007). In this algorithm, all uncertainties (parameters, conceptual model, input, etc.) are mapped onto the parameter ranges as the procedure tries to capture most of the measured data within the 95% prediction uncertainty (95 PPU). Two indices were used to quantify the goodness of calibration/uncertainty performance: the *p* factor, which is the percentage of data bracketed by the 95PPU band (maximum value of 100%) and the *r* factor, which is the average width of the band divided by the standard deviation of the corresponding measured variable.

Model evaluation is essential to verify the robustness of the model. To evaluate the performance of the model for simulating discharge and suspended sediment, the following statistical parameters, which are usually employed in hydrology, were calculated: the Nash-Sutcliffe efficiency parameter (E_{NS}; Nash and Sutcliffe 1970) and the coefficient of determination (R^2). The E_{NS} ranges from −∞ to 1, with 1 denoting a perfect model agreement with observations:

$$E_{NS} = \frac{\sum_{i=1}^{n}\left(Y_{i,\mathrm{sim}} - Y_{i,\mathrm{obs}}\right)^2}{\sum_{i=1}^{n}\left(Y_{i,\mathrm{obs}} - \bar{Y}_{\mathrm{obs}}\right)^2} \tag{1}$$

$$R^2 = \frac{\left(\sum_{i=1}^{n}\left(Y_{i,\mathrm{obs}} - \bar{Y}_{i,\mathrm{obs}}\right)\left(Y_{i,\mathrm{sim}} - \bar{Y}_{\mathrm{sim}}\right)\right)^2}{\sum_{i=1}^{n}\left(Y_{i,\mathrm{obs}} - \bar{Y}_{i,\mathrm{obs}}\right)\sum_{i=1}^{n}\left(Y_{i,\mathrm{sim}} - \bar{Y}_{\mathrm{sim}}\right)^2} \tag{2}$$

where n is the number of observation/simulation data for comparison, $Y_{i,\mathrm{obs}}$ and $Y_{i,\mathrm{sim}}$ are observed and simulated data, respectively, for each time step i (e.g. day or month), and $\bar{Y}_{i,\mathrm{obs}}$ and $\bar{Y}_{i,\mathrm{sim}}$ are the mean values for observed and simulated data during the examination period. The E_{NS} indicates how well the plot of observed values *vs* simulated values is close to the 1:1 line and thus provides an overall indication of goodness of fit; R^2 is the proportion of variation explained by fitting a regression line and is a measure of the strength of a linear relationship between simulated and observed data. We considered 1979–1994 and 1972–1978 as the simulation periods for calibration and validation, respectively. The first 3 years were considered as a warm-up period in which the model was allowed to initialize and approach reasonable initial values for model state variables.

Future climate data

We used 0.5° grids of future climate data available through the Climatic Research Unit of the University of East Anglia (http://www.cru.uea.ac.uk) that are downscaled using the time series of global warming from five GCMs and the observed records (Mitchell *et al.* 2004). We used the data of three GCMs: CGCM2 (coupled global climate model) from the Canadian Centre for Climate Modelling and Analysis; HadCM3 from the Hadley Centre for Climate Prediction and Research; and CSIRO2 from the Australian Commonwealth Scientific and Industrial Research Organization. Scenarios with the highest (A1FI scenario—970 ppm by 2100), lowest (B1 scenario—550 ppm by 2100) and plausible (A2 scenario—845 ppm by 2100) projected CO_2 concentrations were chosen for this study. The monthly maximum temperature, minimum temperature and precipitation are available at global coverage from 2001 to 2100 (Mitchell *et al.* 2004).

Emissions scenarios used in this study are not specific predictions of future climate but are plausible alternative futures. The A1FI scenario assumes a future world of very rapid economic growth, global population that peaks mid-century and declines thereafter, and rapid introduction of new and more efficient technologies. The B1 scenario assumes a convergent world with the same low population growth as in the A1 scenario, but with rapid changes in economic structures toward a service and information economy with reductions in material intensity and the introduction of clean and resource-efficient technologies. The A2 scenario assumes slow development of alternative fuel technologies and prominent fossil fuel usage. We used three scenarios and three GCMs published by the IPCC (IPCC 2007) covering a wide range of uncertainty in global warming in the 21st century. Climate change scenarios were developed using downscaled monthly average precipitation and monthly mean temperature data. The historical baseline time period for comparison of the downscaled climate data with the observed data of precipitation and temperature stations was 1971–2000. (Woznicki *et al.* 2011).

In this study the GCM grid box data were spatially interpolated to the target station using the inverse distance-weighted (IDW) interpolation method using four neighbouring cells. Taking the centre as the grid point for each grid box, we used the following equation to calculate values for each site based on its distance to the geographical centres of the four nearest GCM grid cells:

$$S_i = \sum_{k=1}^{4}\left[\frac{1}{d_{i,k}^{m}}\left(\sum_{j=1}^{4}\frac{1}{d_{i,j}^{m}}\right)^{-1}P_k\right] \tag{3}$$

where S_i is the downscaled site-specific GCM projection at site i, P_k is the GCM projection at the cell k, $d_{i,k}$ is the distance between site i and the centre of cell k and m = 3 (Liu and Zuo 2012). Then we used the change factor (CF) method (Chen *et al.* 2011) to generate climate change scenarios for 2040–2069. The CF method involves adjusting the observed daily temperature ($T_{obs,d}$) by adding the difference in monthly temperature predicted by the climate model (GCM or RCM) between the future horizon and the reference period ($T_{CM,fut,m}$ $T_{CM,ref,m}$) to obtain daily temperature at the future horizon ($T_{adj,fut,d}$) (equation (4)). The adjusted daily precipitation for the future horizon ($P_{adj,fut,d}$) is obtained by multiplying the precipitation ratio ($P_{CM,fut,m}/P_{CM,ref,m}$) with the observed daily precipitation ($P_{obs,d}$) (equation (5)).

$$T_{adj,fut,d} = T_{obs,d} + \left(\bar{T}_{CM,fut,m} - \bar{T}_{CM,ref,m}\right) \tag{4}$$

$$P_{adj,fut,d} = P_{obs,d}\left(\bar{P}_{CM,fut,m}/\bar{P}_{CM,ref,m}\right) \tag{5}$$

Finally, daily data for each GCM under different emission scenarios were developed for each meteorological station and fed into the calibrated and validated SWAT model to project the watershed-scale changes in hydrological components in the 2040–2069 period.

Results and discussion

Model calibration and verification

The SWAT model was calibrated based on daily measured discharge at eight stations and sediment data at six stations within the watershed. Sensitivity analysis using SUFI-2 in the SWAT-CUP was first performed through evaluating the effect of parameters on the performance of the SWAT model in simulating suspended sediment and runoff. Primary results showed that performances of single-gauge calibration were better than multi-gauge in the Gorganroud watershed. Therefore, sensitivity analysis, calibration and validation of the SWAT model were performed for each station separately. Figures 2 and 3 compare graphically measured and simulated monthly streamflow and sediment yield values with the 95PPU band for the calibration and validation period at the Ghazaghli station located near the main outlet.

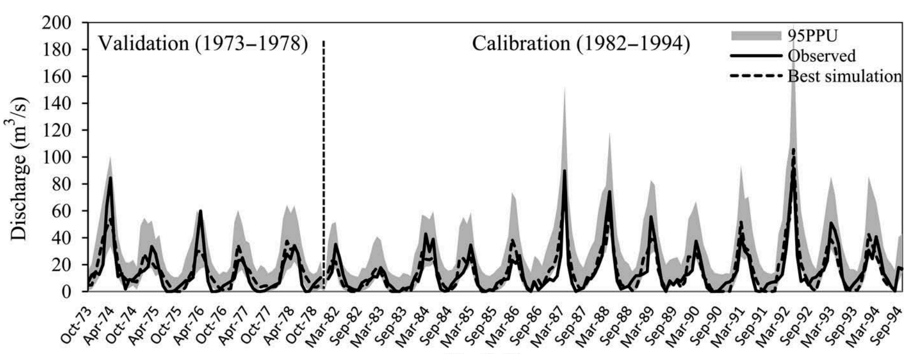

Figure 2. Comparison of the observed, best simulation and 95% prediction uncertainty band for streamflow in Gazaghli station.

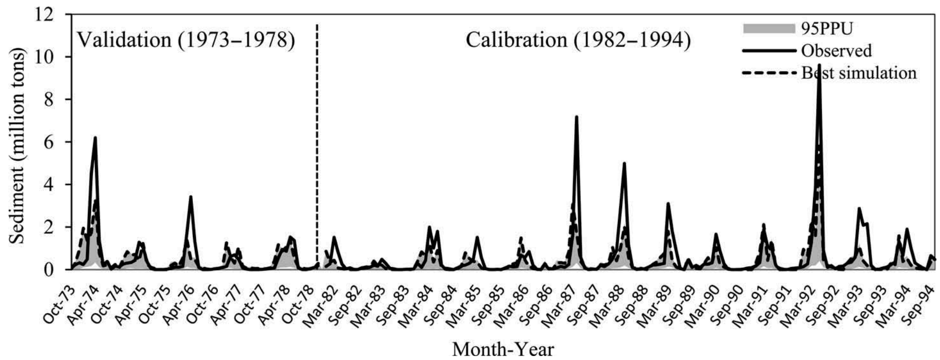

Figure 3. Comparison of the observed, best simulation and 95% prediction uncertainty band for monthly sediment yield in Gazaghli station.

Table 1. Monthly model calibration and validation statistics for stream discharge.

ID in Map	Station	Calibration				Validation			
		p factor	*r* factor	R^2	E_{NS}	*p* factor	*r* factor	R^2	E_{NS}
q005	Tamar	0.63	1.31	0.55	0.49	0.67	1.12	0.49	0.44
q001	Tangrah	0.60	0.89	0.58	0.57	0.52	1.3	0.46	0.44
q011	Gonbad	0.82	1.37	0.73	0.66	0.73	0.98	0.59	0.58
q023	Ghazaghli	0.77	1.17	0.78	0.77	0.76	1.17	0.71	0.70
q019	Arazkoose	0.71	1.23	0.77	0.77	0.70	0.85	0.65	0.65
q007	Galikesh	0.58	0.73	0.5	0.5	0.56	0.67	0.38	0.37
q013	Lazoreh	0.55	0.50	0.58	0.52	0.7	0.7	0.5	0.49
q015	Pasposhteh	0.71	0.79	0.7	0.69	0.58	0.6	0.55	0.54

In addition to the visual comparisons and evaluating the model performance (Figs 2 and 3), numerical criteria including E_{NS}, R^2, *p* factor and *r* factor are presented in Table 1. The E_{NS} for the calibration and validation periods was 0.77 and 0.76 respectively for streamflow in the Ghazaghli station. These results indicated a close relationship between simulated monthly streamflows with measured values. The E_{NS} for upstream stations was not very good except Arazkoose which is located near the main outlet. The conceivable reason contributing to this result may be a weakness of SWAT in simulating the snow melt process in upland areas (Rostamian *et al.* 2008). In general, based on monthly E_{NS} values for the calibration and validation periods and the performance ratings of Moriasi *et al.* (2007) SWAT's performance in simulating streamflow was considered "very good" for the main station.

SWAT's performance in simulating sediment yield was "satisfactory" in all of the stations based on monthly E_{NS} values, except for the Lazoreh for which the performance was "unsatisfactory" (Table 2). In general, the model performance in simulating sediment response was not as good as with stream discharge. The poor model performance in predicting high sediment loads might be attributed to errors in the observed sediment yield data, especially during high flows, and to the models that were used for driving daily sediment yield data from daily discharge. The use of MUSLE in SWAT for simulating sediment also has limitations. Development of the model for annual soil loss from agricultural fields, deriving topographic factor (LS) from DEM, and inadequate description of the channel routing process may be sources of errors (Phan *et al.* 2011, Shrestha *et al.* 2013). It can be also noted that errors in streamflow prediction could cause the

Table 2. Monthly model calibration and validation statistics for sediment yield.

ID in Map	Station	Calibration				Validation			
		p factor	*r* factor	R^2	E_{NS}	*p* factor	*r* factor	R^2	E_{NS}
s005	Tamar	0.54	0.99	0.53	0.46	0.65	0.74	0.74	0.74
s011	Gonbad	0.26	0.33	0.58	0.44	0.27	0.36	0.37	0.29
s023	Ghazaghli	0.62	0.33	0.64	0.61	0.68	0.43	0.55	0.51
s019	Arazkoose	0.55	0.10	0.31	0.11	0.54	0.28	0.44	0.43
s007	Galikesh	0.64	1.39	0.37	0.26	0.64	1.65	0.28	0.25
s013	Lazoreh	0.87	1.38	0.52	0.52	0.48	12.84	0.23	−1.23

discrepancy observed between measured and simulated sediment loads. Overall the model's performance for simulating sediment yield and streamflow was considered satisfactory for conducting the climate change assessment.

Climate change impacts on temperature and precipitation

Mean annual rainfall for all climate stations during the baseline 30-year period (1970–2000) was 553.1 mm and the minimum and maximum yearly rainfall amounts were 320.6 and 856.1 mm, respectively. The average minimum and maximum daily temperatures were 23.0 and 8.5°C, respectively. In Fig. 4 we compared the predicted long-term average precipitation with the historical data for different scenarios. As shown, major changes occur in the spring season (April–June). Figures 5 and 6 show average monthly changes in maximum and minimum temperatures, respectively. Increases in temperature in 2040–2069 for T_{max} in A1F1, A2 and B1 scenarios are 3.3, 2.9 and 2.2°C and for T_{min} are 3.1, 2.1 and 2.7°C, respectively. Monthly variation in temperature in Fig. 5 shows that the maximum increases for T_{max} were predicted in May and June and the minimum increases were predicted in April and November. Whereas maximum increases for T_{min} were predicted in August, September and May, and minimum changes were predicted in November (Fig. 6). In general, all projections showed an increase in temperature over the basin.

Impact of climate change on stream flow

Simulation results projected a decrease in annual streamflow from 14.2% in the A2 scenario of CSIRO2 to an increase of 21.8% in the B1 scenario of HadCM3 for 2040–2069. But in general, the climate change impacts showed an increase in streamflow for this period which has a different temporal pattern in monthly scale depending on the individual scenario and model (Table 3). Average change in annual streamflow in the main outlet was 5.8%, 2.8% and 9.5% for the A1F1, B1 and A2 scenarios, respectively. The study conducted by Abbaspour *et al.* (2009) also reported that climate change may cause more frequent and larger-intensity floods in the wet regions of the country such as Gourganroud in the North of Iran.

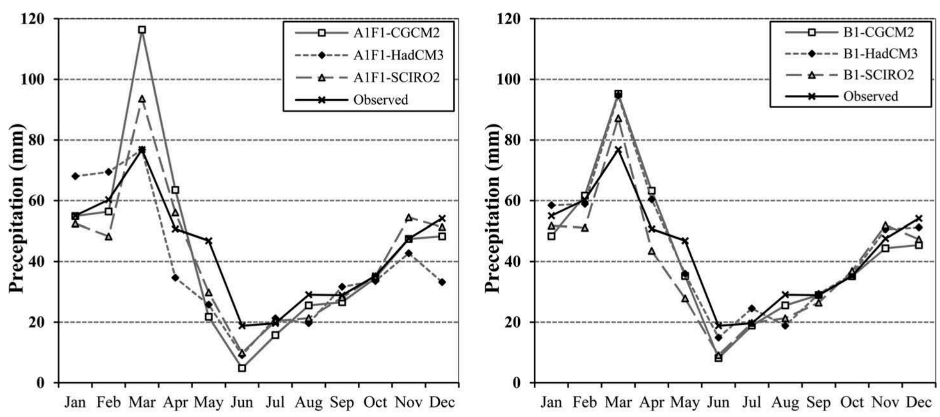

Figure 4. Comparison of average observed monthly precipitation for three GCMs for A1F1 scenario (left) and B1 scenario (right).

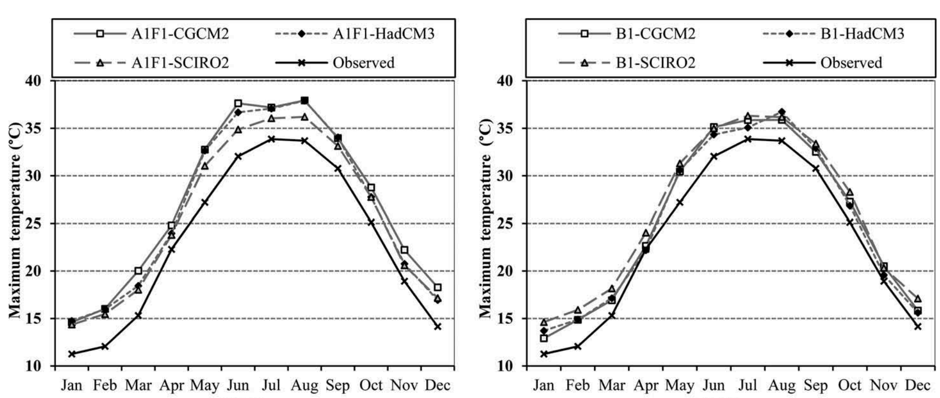

Figure 5. Comparison of maximum temperatures for three GCMs for A1F1 scenario (left) and B1 scenario (right).

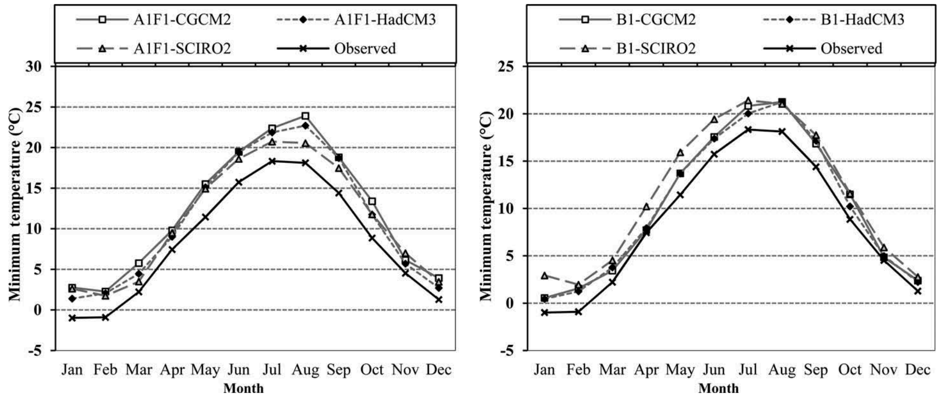

Figure 6. Comparison of minimum temperatures for three GCMs for A1F1 scenario (left) and B1 scenario (right).

Table 3. Predicted relative changes (percent of baseline levels) in monthly streamflow by different GCMs.

Model—scenario	Jan	Feb	Mar	Apr	May	Jun	Jul	Aug	Sep	Oct	Nov	Dec	Average
CGCM2-A1F1	−3.4	−1.0	50.4	59.6	22.1	17.7	−5.5	−15.9	−15.8	−12.0	−2.0	−6.8	19.5
HadCM3-A1F1	−11.9	18.2	9.6	−3.9	−31.5	−33.5	−42.5	−32.8	−11.2	1.9	−15.1	−38.3	−8.9
CSIRO2-A1F1	5.1	−6.7	12.3	25.7	2.8	1.6	−9.0	−16.4	−20.6	−6.4	22.2	22.0	6.9
CGCM2-B1	−17.0	−5.5	23.9	42.1	25.1	23.2	11.8	0.9	2.4	10.8	0.3	−16.7	11.9
HadCM3-B1	10.1	9.0	28.8	41.2	24.7	25.9	36.0	13.3	−4.7	9.8	19.0	12.9	21.8
CSIRO2-B1	−3.5	−7.9	4.0	4.5	−20.0	−20.7	−34.2	−30.6	−32.7	−11.6	22.4	11.8	−5.4
CGCM2-A2	−5.2	−2.6	42.2	54.1	21.0	16.5	−4.6	−17.5	−14.8	−8.4	−0.6	−8.7	16.5
HadCM3-A2	23.4	4.4	10.7	7.6	−22.5	−24.8	−33.3	−28.2	−16.2	26.4	66.7	46.6	6.2
CSIRO2-A2	−12.3	−13.7	−5.8	−6.6	−28.0	−27.6	−36.0	−27.7	−26.8	−13.7	−4.7	−5.4	−14.2

Monthly variations showed that the increase in discharge is more pronounced in March and April and the decrease is more pronounced from the middle of spring until late summer (July–September) (Table 3). Overall, our results showed an increase in annual streamflow which does not occur in dry seasons. Increases in streamflow in wet seasons and decreases in dry seasons were concluded by Rahman *et al.* (2012), Yu and Wang (2009), Phan *et al.* (2011) and Shrestha *et al.* (2013) in different regions. A similar study by Faramarzi *et al.* (2013) for the continent of Africa showed that the mean annual quantity of water resources is likely to increase, but variations are substantial for individual subbasins and countries. Chang and Jung (2010) and Wu *et al.* (2012) also reported that runoff and water yield would increase in spring and substantially decrease in summer.

Figure 7 presents the streamflow probability for the base line and GHGs scenarios for 10 streamflow classes. Study results indicated that climate change may increase the high flows in the region. As shown in Fig. 7, the probability of occurrence of high values in the 10th class (more than 41.8 m^3/s) from the 0.3% baseline has reached 4.9%, 3.3% and 4.1% for the A1F1, A2 and B1 scenarios, respectively, for the period of 2040–2069. Whereas, the probability of occurrence for the most minimum streamflows (less than 7.9 m^3/s) will decrease in this period. These results clearly

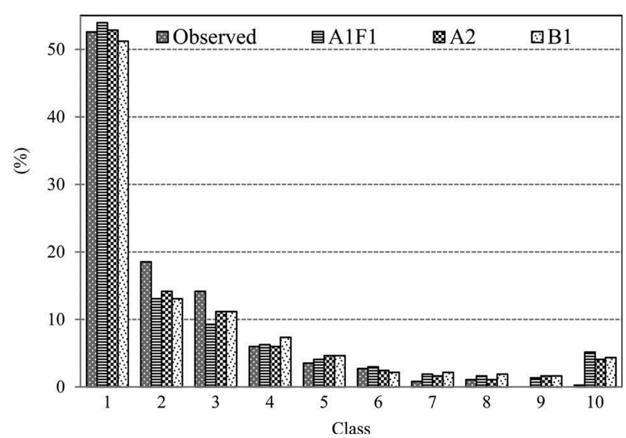

Figure 7. Streamflow probability for base line and GHGs scenarios in different GCMs.

indicate that climate change will threaten water security with more floods and severe scarcity through droughts. Increases in the high flows were also reported in Brazil (Perazzoli *et al.* 2012) and in India (Gosain *et al.* 2006).

Impact of climate change on sediment yield

Prediction of different GCMs showed an increase in sediment yield. This increase varied from nearly 1% (CSIRO2-B1) to 83.9% (CGCM2-A1F1) for annual

Table 4. Predicted relative changes (percent of baseline levels) in monthly sediment yield by different GCMs.

Model—scenario	Jan	Feb	Mar	Apr	May	Jun	Jul	Aug	Sep	Oct	Nov	Dec	Ave.
CGCM2-A1F1	41.4	13.7	286.3	156.0	−48.9	−0.8	−24.2	43.1	38.1	42.9	68.6	6.2	83.9
HadCM3-A1F1	106.7	84.9	49.9	−29.5	−70.5	−49.0	29.0	−39.8	102.4	28.8	1.6	−66.0	25.9
CSIRO2-A1F1	21.8	−22.0	111.5	71.0	−50.6	−39.6	1.3	−35.2	36.7	40.5	125.7	28.4	33.3
CGCM2-B1	31.0	5.2	226.7	141.1	−51.7	−32.6	−29.6	9.3	53.4	32.2	30.6	−4.8	62.9
HadCM3-B1	67.9	−4.8	106.5	−6.3	−69.8	−41.5	19.8	−35.0	80.3	183.2	213.8	71.8	43.9
CSIRO2-B1	0.4	−16.6	54.4	−27.0	−55.2	−45.2	8.6	−29.6	25.9	37.5	45.3	−1.2	0.9
CGCM2-A2	2.8	30.9	132.0	153.8	−19.0	−26.4	−2.1	5.3	50.1	60.2	23.8	−23.1	48.7
HadCM3-A2	47.4	16.5	125.3	116.4	−19.3	−27.7	65.6	−45.5	43.5	61.4	80.2	21.2	54.7
CSIRO2-A2	27.1	−1.4	108.3	12.2	−55.7	−33.0	5.2	−25.5	25.0	78.6	140.1	14.4	30.0

sediment yield (Table 4). In general, the impact of climate change in increasing of sediment yield in the 2040–2069 period was 47.7%, 44.5% and 35.9% for the A1F1, A2 and B1 scenarios, respectively. The increase in sediment yield as a result of climate change was also mentioned by Favis-Mortlock and Guerra (1999), Perazzoli *et al.* (2012) and Nearing *et al.* (2005). Monthly variation showed that the increase in sediment yield in March was the highest with values of 149.2%, 129.4% and 121.9% for the A1F1, A2 and B1 scenarios, respectively. It should be noted that maximum increase in heavy rainfall and extreme events was also predicted in March. Hence, the relative change predicted by the models is reasonable. Overall, different models predicted an increase in sediment yield for all months except May and June.

A comparison of sediment yield predictions and stream discharge predictions for 2040–2069 indicated that the average change in stream discharge for the A1F1, A2 and B1 scenarios were 5.8%, 2.8% and 9.5%, respectively, whereas sediment yield changes were 47.7%, 44.5% and 35.9%, respectively. These results indicated that the impact of climate changes on sediment yield is greater than on streamflow. The relationship between sediment yield and streamflow is usually defined as a power function (Crawford 1991). Considering that the more frequent and larger-intensity floods are prominent features of climate change in the North of Iran, sediment yield changes will be greater than streamflow. The high sensitivity of sediment yield and discharge were also concluded by Zhang *et al.* (2012) and Nunes *et al.* (2009). Therefore climate change impacts on stream discharge and sediment yield may be more significant although these impacts may not be significant for rainfall and temperature.

Figure 8 presents the sediment yield probability for the base line and GHGs scenarios. As shown, the probability of occurrence of high values (last class) from 0.3% for the baseline has reached 5.2%, 4.1% and 4.4% for the A1F1, A2 and B1 scenarios, respectively, for 2040–2069. An increase in high values of

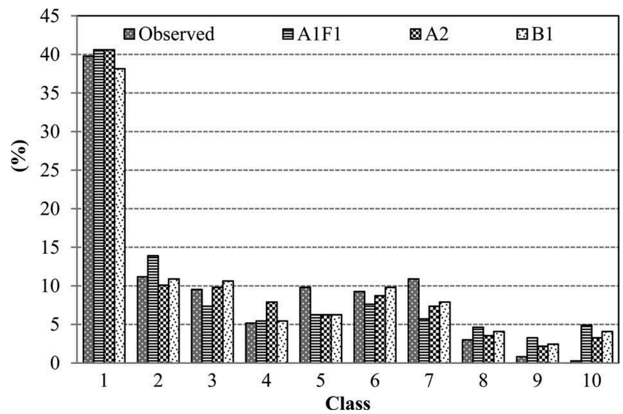

Figure 8. Sediment yield probability for base line and GHGs scenarios in different GCMs.

sediment yield was also reported by Perazzoli *et al.* (2012) in Brazil.

Conclusion

This study assessed the impact of climate change on streamflow and sediment yield in the Gorganroud River basin in the North of Iran. The SWAT hydrological model was used to simulate streamflow and sediment yield and the SUFI-2 algorithm in the SWAT-CUP program was used for parameter optimization. Calibration, validation and uncertainty analysis for both discharge and sediment were generally satisfactory. We used the projections from different climate-change models under different emission scenarios and fed them into the calibrated SWAT model to simulate future changes in discharge and sediment yields due to climate change. Results indicated that differences between the climate model projections in streamflow and sediment yields are high. The study results for 2040–2069 compared with the present climate show increases in annual streamflow of 5.8%, 2.8% and 9.5%, and increases in sediment yield of 47.7%, 44.5% and 35.9% for the A1F1, A2 and B1 scenarios, respectively. This implies that probability of higher increase of sediment yield compared with water flow is high and that the impact of climate changes on sediment yield is greater than on streamflow. Monthly variations showed that the increases in discharge and sediment yield were more pronounced in the wet seasons and decrease in summer (July–September). The results of this study may be helpful to decision makers and other stakeholders for adaptive soil and water resource management practices in a changing climate.

Disclosure statement

No potential conflict of interest was reported by the authors.

References

Abbaspour, K.C., 2007. *User manual for SWAT-CUP, SWAT calibration and uncertainty analysis programs*. Dübendorf, Switzerland: Eawag.

Abbaspour, K.C., *et al*., 2009. Assessing the impact of climate change on water resources in Iran. *Water Resources Research*, 45 (10), W10434. doi:10.1029/2008WR007615

Arnold, J.G., *et al*., 1998. Large area hydrologic modeling and assessment part I: model development. *Journal of the American Water Resources Association*, 34 (1), 73–89. doi:10.1111/j.1752-1688.1998.tb05961.x

Chang, H. and Jung, I.-W., 2010. Spatial and temporal changes in runoff caused by climate change in a complex large river basin in Oregon. *Journal of Hydrology*, 388 (3–4), 186–207. doi:10.1016/j.jhydrol.2010.04.040

Chen, J., Brissette, F.P., and Leconte, R., 2011. Uncertainty of downscaling method in quantifying the impact of climate change on hydrology. *Journal of Hydrology*, 401 (3–4), 190–202. doi:10.1016/j.jhydrol.2011.02.020

Crawford, C.G., 1991. Estimation of suspended-sediment rating curves and mean suspended-sediment loads. *Journal of Hydrology*, 129, 331–348. doi:10.1016/0022-1694(91)90057-O

De Martonne, E., 1926. Aréisme et indice artidite. *Comptes Rendus de l'Académie de Science Paris*, 182, 1395–1398.

Faramarzi, M., *et al*., 2013. Modeling impacts of climate change on freshwater availability in Africa. *Journal of Hydrology*, 480, 85–101. doi:10.1016/j.jhydrol.2012.12.016

Favis-Mortlock, D.T. and Guerra, A.J.T., 1999. The implications of general circulation model estimates of rainfall for future erosion: a case study from Brazil. *Catena*, 37 (3–4), 329–354. doi:10.1016/S0341-8162(99)00025-9

Gosain, A., Rao, S., and Basuray, D., 2006. Climate change impact assessment on hydrology of Indian river basins. *Current Science*, 90 (3), 346–353.

Hamlet, A.F. and Lettenmaier, D.P., 2007. Effects of 20th century warming and climate variability on flood risk in the western U.S. *Water Resources Research*, 43 (6), W06427.

IPCC. 2007. *Climate change 2007: the physical science basis*. Contribution of Working Group I to the Fourth Assessment Report of the Intergovernmental Panel on Climate Change (S.D. Solomon et al., eds.) Cambridge, UK: Cambridge University Press.

Jha, M., *et al*., 2006. Climate change sensitivity assessment on upper Mississippi river basin streamflows using SWAT. *Journal of the American Water Resources Association*, 42 (4), 997–1015. doi:10.1111/j.1752-1688.2006.tb04510.x

Kaini, P., Nicklow, J.W., and Schoof, J.T., 2010. Impact of climate change projections and best management practices on river flows and sediment load. *In: World environmental and water resources congress 2010: challenges of change*. ASCE, 2269–2277. doi:10.1061/41114(371)234

LarConsultingEngineering. 2007. The study on flood and debris flow in the Golestan province. Regional water board in Golestan, Ministry of Energy, Tehran, Iran.

Li, Y., *et al*., 2011. Effects of temperature change on water discharge, and sediment and nutrient loading in the lower pearl river basin based on SWAT modelling. *Hydrological Sciences Journal*, 56 (1), 68–83. doi:10.1080/02626667.2010.538396

Liu, D. and Zuo, H., 2012. Statistical downscaling of daily climate variables for climate change impact assessment over New South Wales, Australia. *Climatic Change*, 115, 629–666. doi:10.1007/s10584-012-0464-y

Mitchell, T.D., *et al*. 2004. A comprehensive set of high-resolution grids of monthly climate for Europe and the globe: the observed record (1901–2000) and 16 scenarios (2001–2100): Tyndall Centre Working Paper.

Moriasi, D., *et al*., 2007. Model evaluation guidelines for systematic quantification of accuracy in watershed simulations. *Transactions of the ASABE*, 50 (3), 885–900. doi:10.13031/2013.23153

Mukundan, R., *et al*., 2013. Suspended sediment source areas and future climate impact on soil erosion and sediment yield in a New York City water supply watershed, USA. *Geomorphology*, 183 (0), 110–119. doi:10.1016/j.geomorph.2012.06.021

Muttiah, R.S. and Wurbs, R.A., 2002. Modeling the impacts of climate change on water supply reliabilities. *Water International*, 27 (3), 407–419. doi:10.1080/02508060208687020

Nash, J.E. and Sutcliffe, J.V., 1970. River flow forecasting through conceptual models part I — a discussion of principles. *Journal of Hydrology*, 10 (3), 282–290. doi:10.1016/0022-1694(70)90255-6

Nearing, M.A., *et al*., 2005. Modeling response of soil erosion and runoff to changes in precipitation and cover. *Catena*, 61 (2–3), 131–154. doi:10.1016/j.catena.2005.03.007

Neitsch, S.L., *et al*., 2005. *Soil and Water Assessment Tool: theoretical documentation*. Temple, TX: USDA-ARS Grassland, Soil and Water Research Laboratory, 476 pp.

Nunes, J.P., *et al*., 2009. Sensitivity of runoff and soil erosion to climate change in two Mediterranean watersheds. Part I: model parameterization and evaluation. *Hydrological Processes*, 23 (8), 1202–1211. doi:10.1002/hyp.7247

Perazzoli, M., Pinheiro, A., and Kaufmann, V., 2012. Assessing the impact of climate change scenarios on water resources in southern Brazil. *Hydrological Sciences Journal*, 58 (1), 77–87.

Phan, D., Wu, C., and Hsieh, S., 2011. Impact of climate change on stream discharge and sediment yield in Northern Viet Nam. *Water Resources*, 38 (6), 827–836. doi:10.1134/S0097807811060133

Rahman, M., Bolisetti, T., and Balachandar, R., 2012. Hydrologic modelling to assess the climate change impacts in a Southern Ontario watershed. *Canadian Journal of Civil Engineering*, 39 (1), 91–103. doi:10.1139/l11-112

Rostamian, R., *et al*., 2008. Application of a SWAT model for estimating runoff and sediment in two mountainous basins in central Iran. *Hydrological Sciences Journal*, 53 (5), 977–988. doi:10.1623/hysj.53.5.977

Shrestha, B., *et al*., 2013. Impact of climate change on sediment yield in the Mekong river basin: a case study of the Nam Ou basin, Lao PDR. *Hydrology and Earth System Sciences*, 17 (1), 1–20. doi:10.5194/hess-17-1-2013

Thodsen, H., Hasholt, B., and Kjærsgaard, J.H., 2008. The influence of climate change on suspended sediment transport in Danish rivers. *Hydrological Processes*, 22 (6), 764–774. doi:10.1002/hyp.6652

Woznicki, S.A., Nejadhashemi, A.P., and Smith, C.M., 2011. Assessing best management practice implementation strategies under climate change scenarios. *Transactions of the ASABE*, 54 (1), 171–190. doi:10.13031/2013.36272

Wu, Y., Liu, S., and Abdul-Aziz, O., 2012. Hydrological effects of the increased CO_2 and climate change in the upper Mississippi river basin using a modified SWAT. *Climatic Change*, 110 (3–4), 977–1003. doi:10.1007/s10584-011-0087-8

Yu, P.-S. and Wang, Y.-C., 2009. Impact of climate change on hydrological processes over a basin scale in northern Taiwan. *Hydrological Processes*, 23 (25), 3556–3568. doi:10.1002/hyp.7456

Zarghami, M., *et al*., 2011. Impacts of climate change on runoffs in East Azerbaijan, Iran. *Global and Planetary Change*, 78 (3–4), 137–146. doi:10.1016/j.gloplacha.2011.06.003

Zhang, Y., *et al*., 2012. Modeling climate change effects on runoff and soil erosion in southeastern Arizona rangelands and implications for mitigation with conservation practices. *Journal of Soil and Water Conservation*, 67 (5), 390–405. doi:10.2489/jswc.67.5.390